Biochimica et Biophysica Acta 1858 (2016) 2208–2214

Contents lists available at ScienceDirect

Biochimica et Biophysica Acta

journal homepage: www.elsevier.com/locate/bbamem

Bacoside-A, an anti-amyloid natural substance, inhibits membrane disruption by the amyloidogenic determinant of prion protein through accelerating fibril formation

Ravit Malishev [a], Sukhendu Nandi [a], Sofiya Kolusheva [b], Shira Shaham-Niv [c], Ehud Gazit [c,d], Raz Jelinek [a,b,*]

[a] Department of Chemistry, Ben Gurion University of the Negev, Beer Sheva 84105, Israel
[b] Ilse Katz Institute for Nanotechnology, Ben Gurion University of the Negev, Beer Sheva 84105, Israel
[c] Department of Molecular Microbiology and Biotechnology, George S. Wise Faculty of Life Sciences, Tel Aviv University, Tel Aviv 69978, Israel
[d] Department of Materials Science and Engineering, Iby and Aladar Fleischman Faculty of Engineering, Tel Aviv University, Tel Aviv 69978, Israel

ARTICLE INFO

Article history:
Received 25 March 2016
Received in revised form 20 June 2016
Accepted 22 June 2016
Available online 27 June 2016

Keywords:
Bacoside
Prion protein
PrP(106–126)
Amyloid peptides
Amyloid fibrils
Membrane interactions

ABSTRACT

Bacosides, class of compounds extracted from the *Bacopa monniera* plant, exhibit interesting therapeutic properties, particularly enhancing cognitive functions and putative anti-amyloid activity. We show that bacoside-A exerted significant effects upon fibrillation and membrane interactions of the amyloidogenic fragment of the prion protein [PrP(106–126)]. Specifically, when co-incubated with PrP(106–126), bacoside-A accelerated fibril formation in the presence of lipid bilayers and in parallel inhibited bilayer interactions of the peptide aggregates formed in solution. These interesting phenomena were studied by spectroscopic and microscopic techniques, which suggest that bacoside A-promoted fibrillation reduced the concentration of membrane-active prefibrillar species of the prion fragment. This study suggests that induction of fibril formation and corresponding inhibition of membrane interactions are likely the underlying factors for ameliorating amyloid protein toxicity by bacoside-A.

1. Introduction

Prion protein (PrP) is the pathogenic substance responsible for transmissible spongiform encephalopathies (TSE), fatal diseases characterized by loss of motor control, dementia, and paralysis [1]. The "prion hypothesis" proposes that native cellular protein PrP (PrP^C), a soluble protein rich in α-helical structures, transforms into the "scrapie form" (PrP^{Sc}), characterized by high β-sheet structures, consequently inducing further aggregation of the native protein [2]. According to this model, the fibrillar aggregates of PrP are responsible for disease initiation and progression [3]. The molecular factors associated with conversion of PrP^C to PrP^{SC} are still not fully resolved, however *cellular membranes* are believed to be intimately involved in the process [4,5]. Furthermore, membrane surfaces might constitute conduits for prion toxicity [6]. Previous studies reveal that membranes and membrane interactions intimately affect the misfolding pathways of amyloidogenic proteins' fibrillation [7–13]. In particular, lipid bilayers have been previously shown both to promote fibrillation of PrP fragments [14–16], as well as constitute a target for binding and interactions of prion aggregates, presumably oligomeric species [17–19].

While virtually all protein-misfolding diseases such as TSE are currently incurable, there is an intense search for therapeutic remedies. In particular, there have been significant efforts towards identification of *small molecules* that are capable of modulating protein aggregation and reduce amyloid protein toxicity [20–23]. *Bacoside A*, mixed saponins that are the active compounds of the medicinal plant *Bacopa monniera*, is used in traditional Indian medicine to treat various nervous disorders and contribute to memory enhancement [24,25]. Recent studies have suggested that bacoside-A might exhibit therapeutic effects against amyloid diseases, such as Alzheimer's disease [26,27].

Here, we investigate the interactions between bacoside-A and the 21-residue amyloidogenic determinant of the prion protein [termed PrP(106–126)] [14,16,17,28]. In particular, we assessed the consequence of bacoside-A/prion interactions upon ***membrane bilayers***. The experimental data reveal acceleration of PrP(106–126) fibril formation in the presence of lipid bilayers. Importantly, we found that he enhanced fibrillation of the peptide, induced by bacoside-A, went hand-in-hand with significantly reduced membrane interactions and bilayer disruption. This work demonstrates a direct relationship between externally-induced accelerated fibrillation and inhibition of membrane interactions, and points to possible use of bacoside-A and

* Corresponding author at: Department of Chemistry, Ben Gurion University of the Negev, Beer Sheva 84105, Israel.
E-mail address: razj@bgu.ac.il (R. Jelinek).

http://dx.doi.org/10.1016/j.bbamem.2016.06.019
0005-2736/

other aggregation modulators as potential therapeutic agents for TSE and amyloid diseases in general.

2. Experimental section

2.1. Materials

PrP(106–126) having the sequence KTNMKHMAGAAAAGAVVGGLG was purchased from Peptron (South Korea) in a lyophilized form at >95% purity (HPLC), bacoside A was purchased from Natural Remedies (Bangalore, India), 1,2-dioleoyl-*sn*-glycero-3-phosphocholine (DOPC), 1,2-dioleoyl-*sn*-glycero-3-phospho-(1′-*rac*-glycerol) (DOPG), 1,2-dimyristoyl-*sn*-glycero-3-phosphocholine (DMPC), 1,2-dimyristoyl-*sn*-glycero-3-[phospho-rac-(1-glycerol)] (DMPG), 1,2-dimyristoyl-*sn*-glycero-3-phosphoethanolamine-*N*-(7-nitro-2-1,3-benzoxadiazol-4-yl) (N-NBD-PE), and 1,2-dimyristoyl-*sn*-glycero-3-phosphoethanolamine-*N*-(lissamine rhodamine B sulfonyl) (N-Rh-PE) were purchased from Avanti Polar Lipids. Thioflavin T (ThT), 1,1,1,3,3,3-hexafluoro-2-propanol (HFIP), sodium hydrosulfite, sodium phosphate monobasic and Dimethyl Sulfoxide (DMSO) were purchased from Sigma-Aldrich (Rehovot, Israel).

2.2. Sample preparation

PrP(106–126) was dissolved in HFIP at a concentration of 2.5 mM and stored at −20 °C until use to prevent aggregation. For each experiment, the solution was thawed, and the required amount was dried by evaporation for 6–7 h to remove the HFIP. The dried peptide sample was dissolved in 10 mM sodium phosphate, pH 7.4, at room temperature. Stock solutions of bacoside A prepared at 2 mM DMSO and diluted into the PrP(106–126) solutions at the required concentrations. All samples used in the experiments contained final DMSO concentration of 0.5% (v/v).

2.3. Thioflavin T (ThT) fluorescence assay

ThT fluorescence measurements were conducted at 25 °C using 96-well path cell culture plates on a Varioskan plate reader (Thermo, Finland). Measurements were made on samples containing 50 μM PrP(106–126) in the absence or presence of different concentrations of bacoside A and in the presence of lipid vesicles (final concentration 1 mM). A 192-μL aliquot of the aggregation reaction was mixed with 48 μL of 100 μM ThT in sodium phosphate, pH 7.4, in each well. The device was programmed to record fluorescence intensity every minute for 1 h. Excitation and emission wavelengths were 440 and 485 nm, respectively. The fluorescence curves were smoothed by using a five-point adjacent averaging.

2.4. Transmission electron microscopy (TEM).

Peptide aliquots (5 μL) from samples used in the ThT experiments (after 15 min incubation) were placed on 400-mesh copper grids covered with a carbon-stabilized Formvar film. Excess solutions were removed following 2 min of incubation, and the grids were negatively stained for 30 s with a 1% uranyl acetate solution. Samples were viewed in an FEI Tecnai 12 TWIN TEM operating at 120 kV.

2.5. Capillary assay

Samples containing 50 μM PrP(106–126) in the absence or presence of 100 μM bacoside A and in the presence of lipid vesicles (final concentration 1 mM) were prepared and immediately inserted into rectangular glass capillaries (CM Scientific, Silsden, UK), sealed and then monitored under light microscope. Images were recorded in time zero and after 30 min.

2.6. Förster resonance energy transfer (FRET)

Small unilamellar vesicles (SUVs, DMPC/DMPG at 1:1 molar ratio) were prepared by dissolving the lipid components in chloroform/ethanol and drying together under vacuum, followed by dissolution in sodium phosphate, pH 7.4, and sonication of the aqueous lipid mixture at room temperature for 10 min using a Sonics vibracell VCX130 ultrasonic cell disrupter. Prior to drying, the lipid vesicles were supplemented with (7-nitro-2-1,3-benzoxadiazol-4-yl)-phosphatydilethanolamine (N-NBD-PE) and *N*-Rhodamine-B-phosphatydilethanolamine (N-Rh-PE) at a 500:1:1 molar ratio, respectively. 50 μM PrP(106–126) in the absence or presence of bacoside-A at 1:2 PrP(106–126)/modulator concentration ratio, respectively, was added to the vesicles (final vesicle concentration 1 mM) at t = 0. Fluorescence emission spectra were acquired at different time points (λex = 469 nm) in the range of 490–650 nm using a Varioskan 96-well plate reader (Thermo, Finland).

To calculate the extent of FRET efficiency the following equation was used:

$$Efficiency = \frac{R_i - R_{100\%}}{R_0 - R_{100\%}} \times 100$$

in which R is a ratio of fluorescence emission of NBD-PE (531 nm)/Rhodamine B-PE (591 nm). Ri is the ratio in the peptide/vesicles mixtures, R100% was measured following the addition of 20% Triton X-100 to the vesicles, which causes complete dissolution of the vesicles, and R_0 corresponds to the ratio recorded for vesicles without any additives.

2.7. Giant unilamellar vesicles labeled with C-dot-DMPC

Amphiphilic carbon dots were prepared according to a published protocol. Briefly, the C-dot labeled lipids were prepared via a phosphorylation reaction between a chloride derivative of dimyristoylphosphatydilcholine (DMPC), a widely-studied membrane lipid [29] and C-dots that were synthesized through a hydrothermal method from 6-*O*-acylated fatty acid ester of D-glucose [30,31].

Giant unilamellar vesicles (GUVs) were prepared through the rapid evaporation method [32]. Briefly, GUVs comprising DOPC and DOPG (1:1 mole ratio) were prepared through dissolving the lipid constituents with 2 mg of C-dots-DMPC dissolved in 500 μL chloroform through vortexing and sonication. The mixture was then transferred to a 250-mL round-bottom flask and the aqueous phase (2.5 mL of 0.1 M sucrose, 0.1 mM KCl, 50 mM Tris solution, pH 7.4) was added carefully with a pipette and stirred gently for ~5 min. The organic solvent was removed in a rotary evaporator under reduced pressure (final pressure 20 mbar) at room temperature. After evaporation for 4–5 min an opalescent fluid was obtained with a volume of approximately 2.5 mL.

2.8. Confocal fluorescence microscopy

GUVs were imaged in the absence or presence of PrP(106–126), bacoside A, or their mixtures using a PerkinElmer UltraVIEW system equipped with an Axiovert-200 M (Zeiss, Germany) microscope and a Plan-Neofluar 63×/1.4 oil objective. The excitation wavelengths of 440 and 488 nm were generated by an Ar/Kr laser.

2.9. Fluorescence anisotropy

The fluorescence probe C-dot-DMPC was incorporated into the SUVs (DOPC/DOPG at 1:1 molar ratio) by adding the dye dissolved in chloroform (0.4 mg/mL) to the lipid and drying together under vacuum, followed by dissolution in sodium phosphate, pH 7.4, and sonication of the aqueous lipid mixture at room temperature for 10 min using a Sonics vibracell VCX130 ultrasonic cell disrupter. The fluorescence emission anisotropy of the C-dot-DMPC fluorescence was measured at

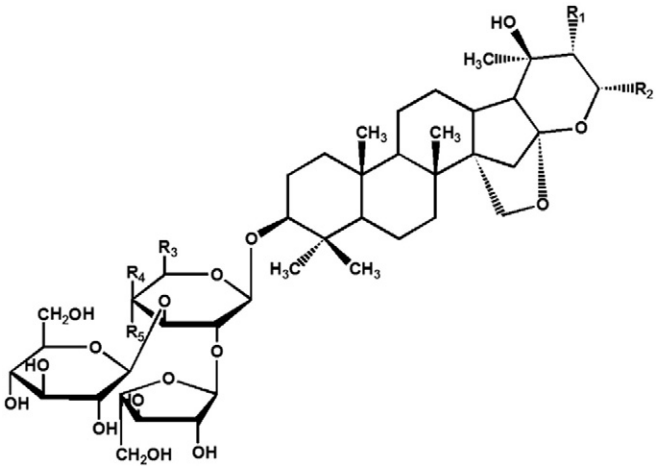

Fig. 1. Molecular structure of bacoside-A. R1–R5 functional units are outlined in Table 1.

463 nm (excitation 375 nm) before and after addition of PrP(106–126), bacoside-A, or their mixture solutions at room temperature on a FL920 spectrofluorimeter (Edinburgh Co., Edinburgh, UK). Anisotropy values were automatically calculated by the spectrofluorimeter software.

3. Results & discussion

Fig. 1 depicts the structure of the bacoside-A backbone. Bacoside-A constitutes a mixture of steroidal saponins; Table 1 outlines the specific composition of the bacoside-A blend employed in the study. Since bacoside-A comprises of a mixture of amphiphilic compounds containing sterol and sugar moieties, one expects that the material would interact with both bilayer membranes as well as amphiphilic peptides. Bacoside-A forms micellar assemblies in organic solvent/water solutions due to the amphiphilic properties (Fig. 1, SI). The spectroscopy and microscopy experiments in Figs. 2–6 were designed to examine whether, and to what extent, bacoside-A interferes with both PrP(106–126) fibrillation as well as with the concurrent bilayer interactions of the peptide assemblies formed throughout the fibrillation process.

Fig. 2 depicts thioflavine-T (ThT) fluorescence curves recorded in different solutions of PrP(106–126) – the peptide in buffer, and co-incubated with vesicle bilayers and bacoside-A in several concentrations. ThT is widely used as a marker for protein fibril formation, as its fluorescence increases upon binding to fibril aggregates comprising strands [33,34]. The ThT fluorescence curves in Fig. 2 reflect significant differences in PrP(106–126) fibrillation rates depending upon both the presence of lipid vesicles and concentrations of bacoside-A co-incubated with the prion fragment. The flat ThT fluorescence curve in Fig. 2i corresponds to PrP(106–126) in a buffer solution *not containing* DMPC/DMPG vesicles, reflecting the very slow fibrillation of the prion fragment when *not* in membrane environments [15,16]. Similar negligible ThT fluorescence signals were recorded in solutions of bacoside A alone or bacoside A in the presence of lipid vesicles (data not shown). In the presence of DMPC/DMPG vesicles, however, PrP(106–126) underwent rapid aggregation, giving rise to a significant increase of ThT fluorescence reaching a plateau after around 30 min (Fig. 2iii).

The ThT fluorescence data in Fig. 2 reveal fibrillation enhancement effect upon co-incubation of PrP(106–126) with bacoside-A. Importantly, bacoside-A was added to PrP(106–126) *before* co-incubation with the lipid vesicles. Specifically, the fluorescence curves in Fig. 2iv–vi point to a direct relationship between the *overall increase* in ThT fluorescence and bacoside-A:PrP(106–126) mole ratio. Furthermore, in the sample comprising 2:1 mole ratio between bacoside-A and PrP(106–126) (Fig. 2, curve vi), both the *rate* of ThT fluorescence increase and absolute intensity were noticeably more pronounced compared to the two other bacoside-A/PrP(106–126) mixtures, confirming that bacoside-A gave rise to enhanced PrP(106–126) fibrillation process. It should be emphasized that the fibrillation enhancement effect was apparent *only in the presence of DMPC/DMPG vesicles*; the flat ThT curve in Fig. 2ii indicates that no fibrillation occurred in a bacoside-A/PrP(106–126) mixture in buffer only (without lipid vesicles).

Microscopy experiments in Fig. 3 provide visual evidence for bacoside-A-induced PrP(106–126) fibrillation. Optical microscopy experiments carried out in a capillary tube [35] reveal pronounced differences in the kinetics of PrP(106–126) fibril formation and morphologies upon co-incubation of the peptide with bacoside-A and its subsequent addition to lipid vesicles (Fig. 3A). Specifically, while no aggregates were apparent in the control sample containing PrP(106–126) and DMPC/DMPG vesicles immediately after their mixing (time = 0 min) (Fig. 3A(i)), short fibers were clearly observed upon addition of bacoside-A/PrP(106–126) mixture to the vesicles (Fig. 3A(ii)). Moreover, Fig. 3A demonstrates that significant differences in PrP(106–126) *aggregate morphologies* were recorded after 30-min incubation. In particular, bacoside-A co-incubation with the prion peptide induced an entangled network of elongated fibers (Fig. 3A(ii)), while a more amorphous peptide aggregate was visualized in the control sample (Fig. 3A(ii)).

Transmission electron microscopy (TEM) experiments depicted in Fig. 3B further illustrate the effect of bacoside-A upon the abundance and morphologies of the PrP(106–126) aggregates. Specifically, thin, dispersed PrP(106–126) fibers were observed in the TEM analysis after 15-minute incubation with DMPC/DMPG vesicles (Fig. 3B(i)). In comparison, Fig. 3B(ii) reveals that co-incubation of *bacoside-A* with PrP(106–126) prior to incubation with the DMPC/DMPG vesicles generated abundant fibrils that were visibly thicker compared to the sample without bacoside-A. More pronounced fibrillation in the mixed samples was similarly apparent in TEM measurements carried out after 60-minute incubation (Fig. 2, SI). Turbidity assay [36] applied to the PrP(106–126)/vesicle and PrP(106–126)/bacoside-A/vesicle solutions, respectively, similarly pointed to enhanced aggregation upon pre-incubation of PrP(106–126) with bacoside-A (Fig. 3, SI).

While Figs. 2 and 3 demonstrate significantly-enhanced bacoside-A-induced fibrillation of PrP(106–126) in the presence of lipid bilayers, an important question one needs to address concerns the effect of bacoside-A upon membrane interactions of the peptide species assembled in solution. This issue is scientifically and therapeutically importance since membrane-active oligomeric and pre-fibril species of amyloid peptides including the prion protein are believed to play prominent roles in the toxicity profiles of these biomolecules and the pathogenicity of amyloid diseases [37–39]. Figs. 4–5 present biophysical analyses of the impact of PrP(106–126)/bacoside-A mixtures upon the structures and dynamics of membrane bilayers.

Table 1
Composition of bacoside-A employed in this study. The molecular composition of bacoside-A was determined by HPLC chromatography and mass spectrometry.

	R1	R2	R3	R4	R5	% W/W
Bacoside A3	H	$CH=C(CH_3)_2$	CH_2OH	H	OH	19.5
Bacopaside II	$CH=C(CH_3)_2$	H	CH_2OH	H	OH	26.9
Jujubogenin isomer of bacopasaponin C	H	$CH=C(CH_3)_2$	H	OH	H	32.3
Bacopasaponin C	$CH=C(CH_3)_2$	H	H	OH	H	17.2

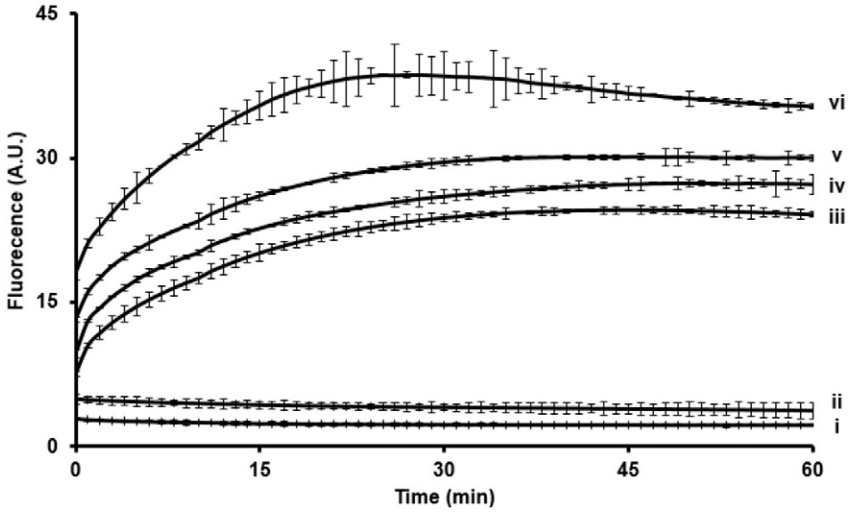

Fig. 2. Fibrillation kinetics of PrP(106–126). ThT fluorescence curves recorded in different PrP(106–126) solutions (peptide concentration was 50 μM). i. PrP(106–126) in *buffer*; ii. PrP(106–126) in *buffer* + addition of bacoside-A (100 μM); iii. PrP(106–126) in the presence of *DMPC/DMPG vesicles* (1 mM); iv. PrP(106–126) pre-incubated with bacoside-A (25 μM) and added to DMPC/DMPG vesicles; v. PrP(106–126) pre-incubated with bacoside-A (50 μM) and added to DMPC/DMPG vesicles; vi. PrP(106–126) pre-incubated with bacoside-A (100 μM) and added to DMPC/DMPG vesicles. All curves represent fluorescence values after subtraction of the background emissions (ThT in buffer or ThT in DMPC/DMPG vesicles). Error bars were calculated from triplicate experiments.

Fig. 4A presents Förster resonance energy transfer (FRET) experiments illuminating the effects of PrP(106–126) and bacoside-A upon DMPC/DMPG vesicles which also contained NBD-PE and Rh-PE as the fluorescence donor and acceptor, respectively. FRET has been previously employed for investigating structural and dynamic modulations within lipid bilayer systems, particularly the effects of membrane-active molecules [40,41]. The pronounced increase in FRET efficiency (i.e. greater intensity of the acceptor fluorescence, F_A, affected by incubation of PrP(106–126) with the NBD-PE/Rh-PE/DMPC/DMPG vesicles (curve i, Fig. 4A), reflects smaller average distance between bilayer-embedded donor and acceptor, likely induced by accumulation of membrane-active peptide aggregates, specifically oligomeric species upon the bilayer surface.

Modification of bilayer interactions of PrP(106–126) was detected, however, when bacoside-A was co-incubated with the prion fragment (Fig. 4A, curve ii). Specifically, the lower FRET efficiency indicates reduction of bilayer binding of PrP(106–126) upon pre-addition of bacoside-A. Indeed, the reduced FRET recorded in case of the PrP(106–126)/mixture is specifically due to interactions between bacoside-A and the amyloidogenic peptide, since bacoside-A alone also gave rise to slight increase in FRET efficiency (Fig. 4A, curve iii).

The fluorescence anisotropy measurements in Fig. 4B corroborate the FRET data and further illuminate the effect of bacoside-A/PrP(106–126) interactions upon bilayer dynamics. Fig. 4B displays the fluorescence anisotropy values of a newly-synthesized carbon-dot (C-dot)-phospholipid conjugate embedded within DMPC/DMPG vesicles; recent reports have shown that C-dots constitute a sensitive fluorescent probe for membrane dynamics and impact of membrane-active molecules [30]. Indeed, Fig. 4B shows that PrP(106–126) individually significantly increased the fluorescence anisotropy of the

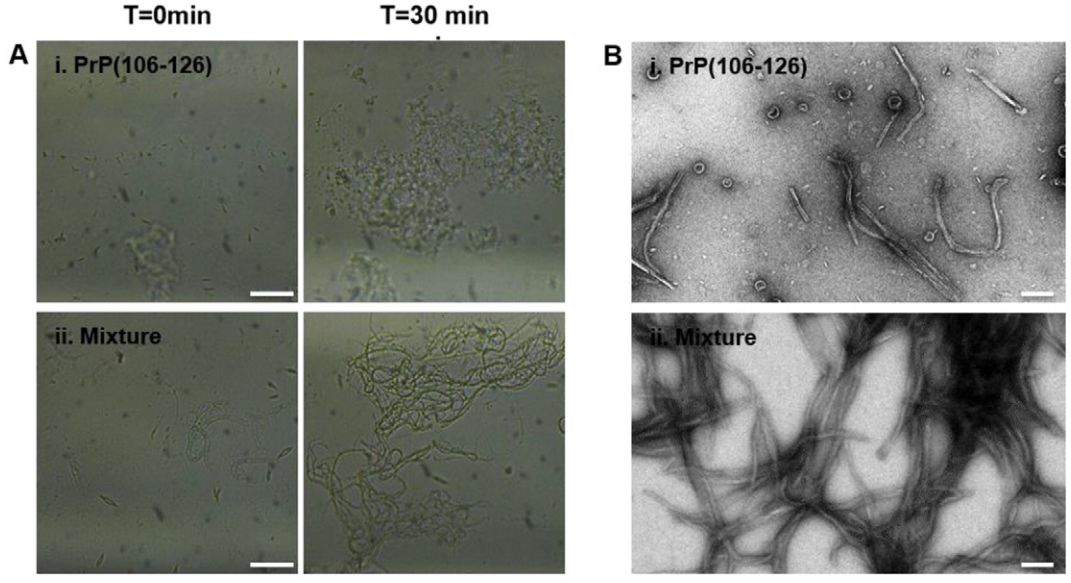

Fig. 3. Microscopy analyses of PrP(106–126) aggregation in the presence of DMPC/DMPG vesicles. A. Capillary-tube optical microscopy. i. Only PrP(106–126) (50 μM) added to the vesicle solution (1 mM); ii. PrP(106–126) (50 μM) pre-incubated with bacoside-A (100 μM) added to the vesicle solution. Scale bar corresponds to 25 μm. B. Transmission electron microscopy (TEM) images of the tested samples after 15 min incubation. i. 50 μM PrP(106–126) added to the vesicle solution (1 mM); ii. 50 μM PrP(106–126) pre-incubated with 100 μM bacoside-A added to the vesicle solution (1 mM). Scale bars in all images correspond to 25 μm.

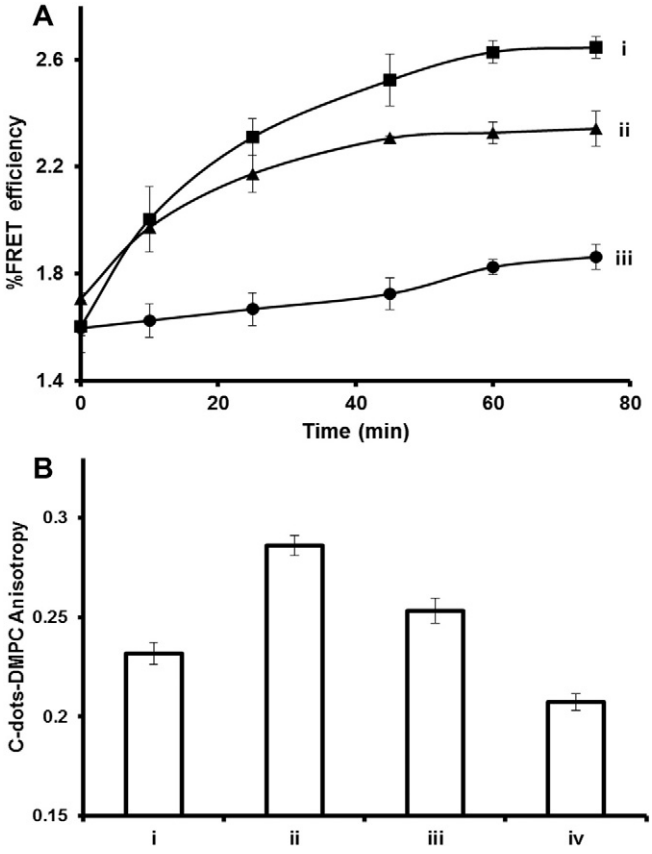

Fig. 4. Effect of bacoside-A upon bilayer dynamics properties. A. Förster resonance energy transfer (FRET) efficiency measured in NBD-PE/Rh-PE/DMPC/DMPG vesicles (1:1:500:500 mole ratio). FRET efficiency value of 1 corresponds to the control vesicles prior to addition of either the peptide or bacoside-A. i. 50 μM PrP(106–126) added to the vesicles; ii. 100 μM bacoside-A added to the vesicles; iii. 50 μM PrP(106–126) pre-incubated with 100 μM bacoside-A then added to the vesicles. Error bars were calculated from triplicate experiments. B. Fluorescence anisotropy recorded in C-dot-DMPC/DOPC/DOPG vesicles after 5-min incubation. i. Control vesicles [without addition of PrP(106–126) and bacoside-A]; ii. 50 μM PrP(106–126) added; iii. 50 μM PrP(106–126) and 100 μM bacoside-A mixture added; iv. 100 μM bacoside-A added. Error bars were calculated from triplicate experiments.

vesicle-displayed C-dots, from 0.22 (in the control C-dot-phospholipid/DMPC/DMPG vesicles) to around 0.30. The higher anisotropy corresponds to a *more rigid* bilayer, consistent with the FRET data in Fig. 4A which revealed immobilization of the acceptor and donor dyes following bilayer interactions of PrP(106–126). Fig. 4B also demonstrates that co-addition of bacoside-A and PrP(106–126) gave rise to significantly lower anisotropy (bar iii). The reduced rigidity cannot be explained simply by an additive effect of bacoside-A (Fig. 4B(iv)). Indeed, the greater bilayer fluidity apparent upon incubating the bacoside-A/PrP(106–126) mixture with the vesicles likely reflects bacoside-A-induced inhibition of PrP(106–126) interactions with the bilayer.

To further probe the inhibitory effect of bacoside-A upon membrane interactions of PrP(106–126) we carried out fluorescence confocal microscopy experiments using giant unilamellar vesicles GUVs) comprising DOPC/DOPG and the C-dot-DMPC fluorescent probe (Fig. 5). The representative confocal microscopy images in Fig. 5 dramatically visualize both the consequences of vesicle interactions of PrP(106–126) and bacoside-A separately, as well as the inhibitory effect of co-incubating the molecules prior to their addition to the GUVs.

Specifically, Fig. 5i reveals "fraying" of the vesicle surface few minutes after addition of PrP(106–126) to the fluorescently C-dot-labeled GUVs. This bilayer disruption is consistent with bilayer association of the peptide recorded both in the FRET and fluorescence anisotropy experiments in Fig. 4. Interestingly, bacoside-A induced significant rearrangement within the vesicle surface, generating dark domains presumably due to significant lipid rearrangement upon bacoside-A binding (Fig. 5ii). This result is consistent with membrane binding of bacoside-A reflected in the fluorescence spectroscopy data in Fig. 4.

In contrast to the modulation of vesicle morphology and surface organization induced by PrP(106–126) and bacoside-A when each was added *separately*, pre-mixing of both molecules and subsequent addition to the C-dot-labeled GUVs did not have discerned structural effect upon the vesicles (Fig. 5iii). The confocal fluorescence microscopy images in Fig. 5iii corroborate the spectroscopy experiments highlighted in Fig. 4, and confirm the "membrane-protective" effect of bacoside-A, when co-incubated with PrP(106–126) prior to addition to the vesicles. Importantly, the inhibitory action of bacoside-A was recorded only upon mixing with PrP(106–126) *prior* to incubation with vesicle bilayers (e.g. Fig. 5iii). An experiment in which bacoside-A was added to a

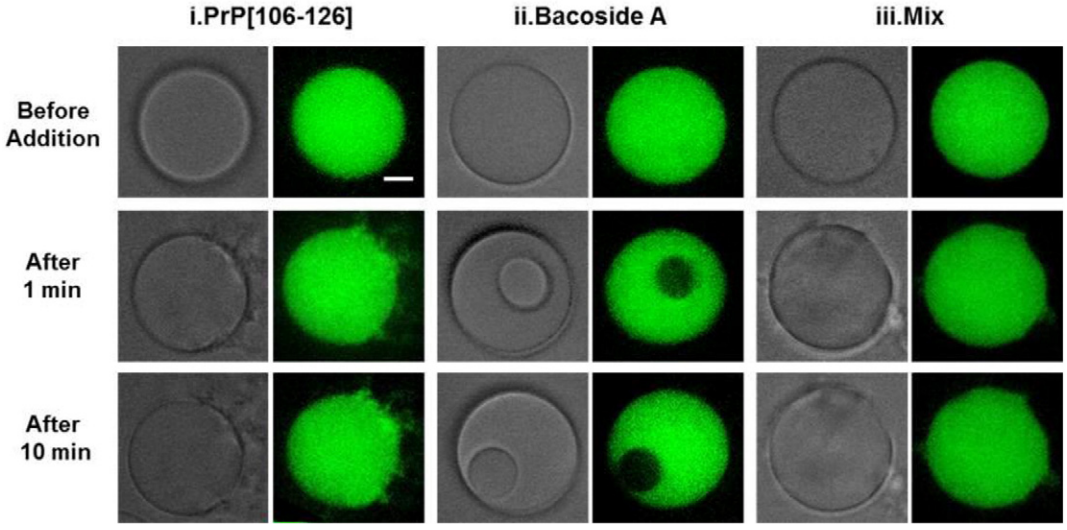

Fig. 5. Visualization of bilayer interactions using giant unilamellar vesicles (GUVs) labeled with a C-dot-phospholipid conjugate. Representative confocal fluorescence microscopy images (Ex 405 nm, emission 440/60) following addition of: i. 50 μM PrP(106–126); ii. 100 μM bacoside-A; iii. 50 μM PrP(106–126) pre-incubated with 100 μM bacoside-A. The left columns depict the corresponding bright-field microscopy images. Scale bar corresponds to 5 μm.

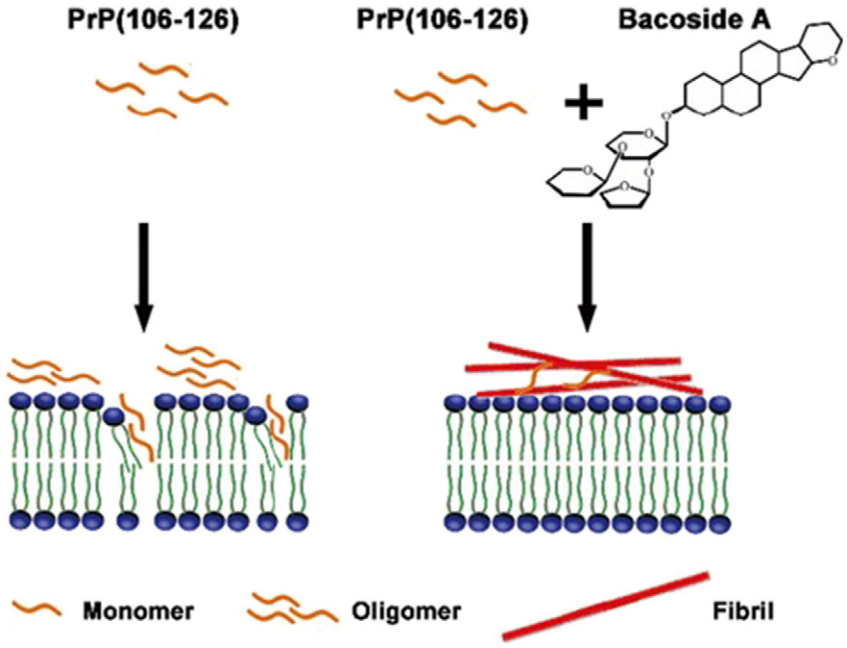

Fig. 6. Schematic model for the activity of bacoside-A. Left: PrP(106–126) *alone* forms abundant pre-fibril aggregates which interact with, and disrupt membrane bilayers; right: when PrP(106–126) is pre-incubated with bacoside-A, fibrillation is accelerated resulting in lower abundance of membrane-active species.

solution in which PrP(106–126) was already mixed with GUVs yielded no interference with membrane interactions of the amyloidogenic peptide (Fig. 4, SI). Moreover, enhancement of the fluorescence within the circular domains was apparent when PrP(106–126) was added to the GUVs *after* first incubation with bacoside-A, possibly due to modulation of bacoside-A-induced lipid reorganization affected by addition of PrP(106–126). These data confirm that specific interactions between PrP(106–126) and bacoside-A are responsible for shielding the bilayer from further interactions by membrane-active soluble species. Isothermal titration calorimetry measurements depicted in Fig. 5, SI indeed demonstrate that when bacoside-A and PrP(106–126) were mixed and subsequently added to lipid bilayers, the molecules interacted with each other, rather than with the membrane bilayers.

The fibrillation kinetics experiments in Figs. 2–3 and membrane interaction analysis in Figs. 4–5 point to a putative mechanism for the effect of bacoside-A upon PrP(106–126), outlined in Fig. 6. At the core of bacoside-A action is *acceleration* of PrP(106–126) fibrillation in the presence of lipid membranes. This process, clearly recorded in the ThT fluorescence and microscopy experiments in Figs. 2 and 3, likely results in *lower abundance* of early-fibril intermediates which are membrane-active and believed to constitute the primary toxic species in amyloid systems [42]. Oligomeric and pre-fibrillar PrP species are indeed believed to play prominent roles in the toxicity of the protein [19,43,44]. Consistent with this interpretation, bacoside-A-induced *inhibition* of lipid-bilayer binding and disruption by PrP(106–126), schematically outlined in Fig. 6, is the most significant experimental result obtained through application of complementary spectroscopic and microscopic techniques (Figs. 4–5).

Overall, the following model, based upon the complementary experiments carried out, is proposed. When PrP(106–126) and bacoside A were mixed and incubated with lipid vesicles, enhanced fibrillation occurred [ThT data in Fig. 2 and microscopy results in Fig. 3]. This process is ascribed to formation of PrP(106–126) aggregation nuclei initially induced by the lipid bilayers (a phenomenon observed in varied amyloid peptide systems), further promoted upon interaction with bacoside-A. Importantly, the *fibril species* that rapidly assembled upon, or close to the membrane surface (Fig. 6, right) effectively *shielded* the membrane from interactions of soluble species – in the case here PrP(106–126). It should be noted that the lipid membranes were likely pivotal in promoting interactions between PrP(106–126) and bacoside A; no interactions between the two species were apparent in the ITC analysis (data not shown).

4. Conclusions

In conclusion, this study examined the effect of bacoside-A, a natural substance exhibiting anti-amyloid toxicity properties, upon membrane interactions and bilayer-induced fibrillation of PrP(106–126), the amyloidogenic determinant of the prion protein. The experimental data reveal that pre-incubation of PrP(106–126) with bacoside-A prior to addition to vesicle bilayers clearly enhanced fibril formation, and in parallel inhibited membrane interactions of the peptide assemblies. The bacoside-A-induced aggregate acceleration and reduced bilayer interactions are likely ascribed to lower concentration of membrane-active early-fibril PrP(106–126) species. While bacoside-A has not been studied yet in conjunction with the prion protein, the results reported here point to significant interactions of the compound with the amyloidogenic determinant of PrP, and apparent effects upon the structural and functional properties of the peptide. In a broader context, the anti-amyloid properties of bacoside-A might be traced to its effect in reducing the concentration of membrane-active, toxic peptide species through promoting and enhancing fibrillation.

Conflict of interest statement

There is no financial/personal interest or belief that could affect the objectivity of the authors.

There is no conflict of interest.

Transparency document

The Transparency document associated with this article can be found, in the online version.

Acknowledgements

We are grateful to Dr. Hao Jiang for the help with modeling.

Appendix A. Supplementary data

DLS data for bacoside A in DMSO/water solution. TEM images of PrP(106-126) and PrP(106-126)/bacoside A with DMPG/DMPC vesicles. Turbidity data of PrP(106-126)/vesicles and PrP(106-126)/bacoside-A/vesicles. Confocal fluorescence microscopy images of GUVs following interactions with PrP(106-126) and bacoside A. ITC data for vesicle solutions containing PrP(106-126), Bacoside A, their mixture and buffer alone. Supplementary data to this article can be found online at http://dx.doi.org/10.1016/j.bbamem.2016.06.019.

References

[1] B.K. Nimiwal, M.K. Jalandhra, M. Sharma, S. Thacker, Prion protein as a pathogen: a review, Int. J. Biomed. Adv. Res. 3 (2012) 531–536.
[2] N.R. Cashman, B. Caughey, Prion diseases—close to effective therapy? Nat. Rev. Drug Discov. 3 (2004) 874–884.
[3] B. Frost, M.I. Diamond, Prion-like mechanisms in neurodegenerative diseases, Nat. Rev. Neurosci. 11 (2010) 155–159.
[4] N. Sanghera, T.J. Pinheiro, Binding of prion protein to lipid membranes and implications for prion conversion, J. Mol. Biol. 315 (2002) 1241–1256.
[5] M. Stefani, Biochemical and biophysical features of both oligomer/fibril and cell membrane in amyloid cytotoxicity, FEBS J. 277 (2010) 4602–4613.
[6] S. Noinville, J.-F. Chich, H. Rezaei, Misfolding of the prion protein: linking biophysical and biological approaches, Vet. Res. 39 (2008) 1–17.
[7] G.P. Gorbenko, P.K. Kinnunen, The role of lipid–protein interactions in amyloid-type protein fibril formation, Chem. Phys. Lipids 141 (2006) 72–82.
[8] M.S. Terakawa, H. Yagi, M. Adachi, Y.-H. Lee, Y. Goto, Small liposomes accelerate the fibrillation of amyloid β (1–40), J. Biol. Chem. 290 (2015) 815–826.
[9] S. Cote, V. Binette, E.S. Salnikov, B. Bechinger, G. Wei, N. Mousseau, Oligomerization of huntingtin N-terminal fragment on a phospholipid bilayer revealed by molecular dynamics simulations, Biophys. J. 106 (2014) 99a–100a.
[10] J.R. Brender, U.H. Dürr, D. Heyl, M.B. Budarapu, A. Ramamoorthy, Membrane fragmentation by an amyloidogenic fragment of human islet amyloid polypeptide detected by solid-state NMR spectroscopy of membrane nanotubes, Biochim. Biophys. Acta Biomembr. 1768 (2007) 2026–2029.
[11] R.M. Murphy, Kinetics of amyloid formation and membrane interaction with amyloidogenic proteins, Biochim. Biophys. Acta Biomembr. 1768 (2007) 1923–1934.
[12] C. Cecchi, M. Stefani, The amyloid-cell membrane system. The interplay between the biophysical features of oligomers/fibrils and cell membrane defines amyloid toxicity, Biophys. Chem. 182 (2013) 30–43.
[13] C.I. Yang, B.N. Tsai, S.J. Huang, T.Y. Wang, H.C. Tai, J.C. Chan, Aggregation of beta-amyloid peptides proximal to zwitterionic lipid bilayers, Chem. – Asian J. 10 (2015) 1967–1971.
[14] J. Dorosz, R. Volinsky, E. Bazar, S. Kolusheva, R. Jelinek, Phospholipid-induced fibrillation of a prion amyloidogenic determinant at the air/water interface, Langmuir 25 (2009) 12501–12506.
[15] N. Gal, A. Morag, S. Kolusheva, R. Winter, M. Landau, R. Jelinek, Lipid bilayers significantly modulate cross-fibrillation of two distinct amyloidogenic peptides, J. Am. Chem. Soc. 135 (2013) 13582–13589.
[16] I. Dupiereux, W. Zorzi, L. Lins, R. Brasseur, P. Colson, E. Heinen, B. Elmoualij, Interaction of the 106–126 prion peptide with lipid membranes and potential implication for neurotoxicity, Biochem. Biophys. Res. Commun. 331 (2005) 894–901.
[17] T. Miura, M. Yoda, N. Takaku, T. Hirose, H. Takeuchi, Clustered negative charges on the lipid membrane surface induce β-sheet formation of prion protein fragment 106–126, Biochemistry 46 (2007) 11589–11597.
[18] J. Kazlauskaite, N. Sanghera, I. Sylvester, C. Vénien-Bryan, T.J. Pinheiro, Structural changes of the prion protein in lipid membranes leading to aggregation and fibrillization, Biochemistry 42 (2003) 3295–3304.
[19] P. Walsh, J. Yau, K. Simonetti, S. Sharpe, Morphology and secondary structure of stable β-oligomers formed by amyloid peptide PrP (106 − 126), Biochemistry 48 (2009) 5779–5781.
[20] Y. Cordeiro, L.M.T. Lima, M.P. Gomes, D. Foguel, J.L. Silva, Modulation of prion protein oligomerization, aggregation, and β-sheet conversion by 4, 4′-dianilino-1, 1′-binaphthyl-5, 5′-sulfonate (bis-ANS), J. Biol. Chem. 279 (2004) 5346–5352.
[21] C. Haass, D.J. Selkoe, Soluble protein oligomers in neurodegeneration: lessons from the Alzheimer's amyloid β-peptide, Nat. Rev. Mol. Cell Biol. 8 (2007) 101–112.
[22] J. Bieschke, M. Herbst, T. Wiglenda, R.P. Friedrich, A. Boeddrich, F. Schiele, D. Kleckers, J.M.L. del Amo, B.A. Grüning, Q. Wang, Small-molecule conversion of toxic oligomers to nontoxic β-sheet-rich amyloid fibrils, Nat. Chem. Biol. 8 (2012) 93–101.
[23] N. Lorenzen, S.B. Nielsen, Y. Yoshimura, B.S. Vad, C.B. Andersen, C. Betzer, J.D. Kaspersen, G. Christiansen, J.S. Pedersen, P.H. Jensen, How epigallocatechin gallate can inhibit α-synuclein oligomer toxicity in vitro, J. Biol. Chem. 289 (2014) 21299–21310.
[24] N. Limpeanchob, S. Jaipan, S. Rattanakaruna, W. Phrompittayarat, K. Ingkaninan, Neuroprotective effect of *Bacopa monnieri* on beta-amyloid-induced cell death in primary cortical culture, J. Ethnopharmacol. 120 (2008) 112–117.
[25] S.R. Bammidi, S.S. Volluri, S.C. Chippada, S. Avanigadda, M. Vangalapati, A review on pharmacological studies of *Bacopa monniera*, J. Chem. Biol. Phys. Sci. (JCBPS) 1 (2011) 250.
[26] N. Apetz, G. Munch, S. Govindaraghavan, E. Gyengesi, Natural Compounds and Plant Extracts as Therapeutics Against Chronic Inflammation in Alzheimer's Disease—A Translational Perspective, CNS & Neurological Disorders-Drug Targets (Formerly Current Drug Targets-CNS & Neurological Disorders), 13 2014, pp. 1175–1191.
[27] L.A. Holcomb, M. Dhanasekaran, A.R. Hitt, K.A. Young, M. Riggs, B.V. Manyam, Bacopa monniera extract reduces amyloid levels in PSAPP mice, J. Alzheimers Dis. 9 (2006) 243–251.
[28] F. Tagliavini, F. Prelli, L. Verga, G. Giaccone, R. Sarma, P. Gorevic, B. Ghetti, F. Passerini, E. Ghibaudi, G. Forloni, Synthetic peptides homologous to prion protein residues 106-147 form amyloid-like fibrils in vitro, Proc. Natl. Acad. Sci. 90 (1993) 9678–9682.
[29] D. Marquardt, J.A. Williams, J.J. Kinnun, N. Kucerka, J. Atkinson, S.R. Wassall, J. Katsaras, T.A. Harroun, DMPC: a remarkable exception to the tocopherol's membrane presence, Biophys. J. 106 (2014) 41a.
[30] S. Nandi, R. Malishev, K.P. Kootery, Y. Mirsky, S. Kolusheva, R. Jelinek, Membrane analysis with amphiphilic carbon dots, Chem. Commun. 50 (2014) 10299–10302.
[31] S. Nandi, R. Malishev, S.K. Bhunia, S. Kolusheva, J. Jopp, R. Jelinek, Lipid-Bilayer Dynamics Probed by a Carbon Dot-Phospholipid Conjugate, Biophysical Journal, 110, 2016.
[32] N. Gal, D. Malferarri, S. Kolusheva, P. Galletti, E. Tagliavini, R. Jelinek, Membrane interactions of ionic liquids: possible determinants for biological activity and toxicity, Biochim. Biophys. Acta Biomembr. 1818 (2012) 2967–2974.
[33] M.R. Krebs, E.H. Bromley, A.M. Donald, The binding of thioflavin-T to amyloid fibrils: localisation and implications, J. Struct. Biol. 149 (2005) 30–37.
[34] M. Biancalana, S. Koide, Molecular mechanism of thioflavin-T binding to amyloid fibrils, Biochimica et Biophysica Acta (BBA)-proteins and Proteomics 1804 (2010) 1405–1412.
[35] A. Levin, T.O. Mason, L. Adler-Abramovich, A.K. Buell, G. Meisl, C. Galvagnion, Y. Bram, S.A. Stratford, C.M. Dobson, T.P. Knowles, Ostwald's rule of stages governs structural transitions and morphology of dipeptide supramolecular polymers, Nat. Commun. 5 (2014).
[36] M.F. Jobling, L.R. Stewart, A.R. White, C. McLean, A. Friedhuber, F. Maher, K. Beyreuther, C.L. Masters, C.J. Barrow, S.J. Collins, The hydrophobic core sequence modulates the neurotoxic and secondary structure properties of the prion peptide 106–126, J. Neurochem. 73 (1999) 1557–1565.
[37] R. Malishev, S. Nandi, S. Kolusheva, Y. Levi-Kalisman, F.-G. Klärner, T. Schrader, G. Bitan, R. Jelinek, Toxicity inhibitors protect lipid membranes from disruption by Aβ42, ACS Chem. Neurosci. 6 (2015) 1860–1869.
[38] F. Chiti, C.M. Dobson, Protein misfolding, functional amyloid, and human disease, Annu. Rev. Biochem. 75 (2006) 333–366.
[39] D. Eisenberg, M. Jucker, The amyloid state of proteins in human diseases, Cell 148 (2012) 1188–1203.
[40] L.M. Loura, R.F. de Almeida, M. Prieto, Detection and characterization of membrane microheterogeneity by resonance energy transfer, J. Fluoresc. 11 (2001) 197–209.
[41] N. Gal, S. Kolusheva, N. Kedei, A. Telek, T.A. Naeem, N.E. Lewin, L. Lim, P. Mannan, S.H. Garfield, S. El Kazzouli, *N*-methyl-substituted fluorescent DAG–indololactone isomers exhibit dramatic differences in membrane interactions and biological activity, Chembiochem 12 (2011) 2331–2340.
[42] M. Cheon, I. Chang, S. Mohanty, L.M. Luheshi, C.M. Dobson, M. Vendruscolo, G. Favrin, Structural reorganisation and potential toxicity of oligomeric species formed during the assembly of amyloid fibrils, PLoS Comput. Biol. 3 (2007), e173.
[43] R. Kayed, E. Head, J.L. Thompson, T.M. McIntire, S.C. Milton, C.W. Cotman, C.G. Glabe, Common structure of soluble amyloid oligomers implies common mechanism of pathogenesis, Science 300 (2003) 486–489.
[44] R. Kayed, Y. Sokolov, B. Edmonds, T.M. McIntire, S.C. Milton, J.E. Hall, C.G. Glabe, Permeabilization of lipid bilayers is a common conformation-dependent activity of soluble amyloid oligomers in protein misfolding diseases, J. Biol. Chem. 279 (2004) 46363–46366.